Letter

Ising fracton spin liquid on the honeycomb lattice

Benedikt Placke,[1,*] Owen Benton,[1,2,†] and Roderich Moessner[1,‡]
[1]*Max Planck Institute for the Physics of Complex Systems, Nöthnitzer Straße 38, 01187 Dresden, Germany*
[2]*School of Physical and Chemical Sciences, Queen Mary University of London, London E1 4NS, United Kingdom*

(Received 4 July 2023; revised 5 February 2024; accepted 18 June 2024; published 1 July 2024)

We study a classical Ising model on the honeycomb lattice with local two-body interactions and present strong evidence that at low temperature it realizes a higher-rank Coulomb liquid with fracton excitations. We show that the excitations are (type-I) fractons, appearing at the corners of membranes of spin flips. Because of the threefold rotational symmetry of the honeycomb lattice, these membranes can be locally combined such that no excitations are created, giving rise to a set of ground states described as a liquid of membranes. We devise a cluster Monte Carlo algorithm purposefully designed for this problem that moves pairs of defects, and use it to study the finite-temperature behavior of the model. We show evidence for a first order transition from a high-temperature paramagnet to a low-temperature phase whose correlations precisely match those predicted for a higher-rank Coulomb phase.

DOI: 10.1103/PhysRevB.110.L020401

One of the central concepts in condensed matter physics is the notion of quasiparticles: the idea that the low energy excitations of a system are weakly interacting particlelike objects. In general, these quasipaticles are capable of independent motion, and it is via this motion that energy inserted locally into the system can spread out, thus allowing equilibration. Fractons are quasiparticles outside this paradigm, being completely immobile when isolated [1–11]. Fractons are intimately connected with the conservation laws of exotic gauge theories involving not only charge but higher moments (e.g., dipole moment) of the charge density [12–16]. It is these conservation laws which render isolated fractons immobile.

Recent years have seen a concerted effort to establish theoretical models in which higher moment conservation laws and fracton physics appear [17–25]. Various lattice models have been proposed to give rise to fractonic behavior, although these often require complicated multibody interactions. From the point of view of identifying routes to experimental realization, it is preferable to find models built from short-ranged, two body interactions.

One setting in which the construction of such models has been successful is classical spin systems [26–28]. Classical models have some advantages: a Hamiltonian can be readily constructed to enforce a local constraint of choice in the low energy sector, and this constraint can be chosen in such a way as to reproduce the Gauss's law(s) of a given gauge theory. Once the model is constructed, it is in principle accessible to Monte Carlo simulation.

Successful constructions of such models have so far been restricted to continuous degrees of freedom. Considering instead models of discrete Ising spins presents considerable advantages and, unfortunately, challenges. First, for discrete systems the precise identification of local fractonic excitations is straightforward (in rough analogy to the ease of identifying domain walls in Ising chains), greatly facilitating study of their properties. Second, adding quantum dynamics in a controlled way is then relatively straightforward, by identifying the simplest "resonance" processes between the discrete states in question, again in analogy to the introduction of transverse fields to frustrated Ising models [29].

The challenge is posed by the greatly increased difficulty in numerical studies of Ising models—the limited mobility of the discrete localized fractons effectively prevents local algorithms from reaching equilibrium.

In this letter, we present an Ising model exhibiting a fractonic spin liquid regime. The low temperature behavior of our model is quite distinct from previously discussed fracton models. The ground state ensemble appears to be truly liquidlike, being strongly correlated but without long range ordering, and with an extensive residual entropy. This extensive, as opposed to subextensive (i.e., $\propto$ the number of spins/volume of the system, rather than its linear size), ground state entropy distinguishes it both from previous discrete classical models [21,30] and from fracton topological order [8]. We identify its discrete and local fracton excitations. These appear at the corners of membranes of flipped spins, and can be understood as charges of a higher-rank U(1) gauge theory, distinct from the fractal order discussed in [23].

In order to simulate the model's properties we devise a cluster algorithm for Monte Carlo simulations of fractons, which is purpose built for the study of fractonic Ising models.

*Contact author: placke@pks.mpg.de
†Contact author: j.o.benton@qmul.ac.uk
‡Contact author: moessner@pks.mpg.de

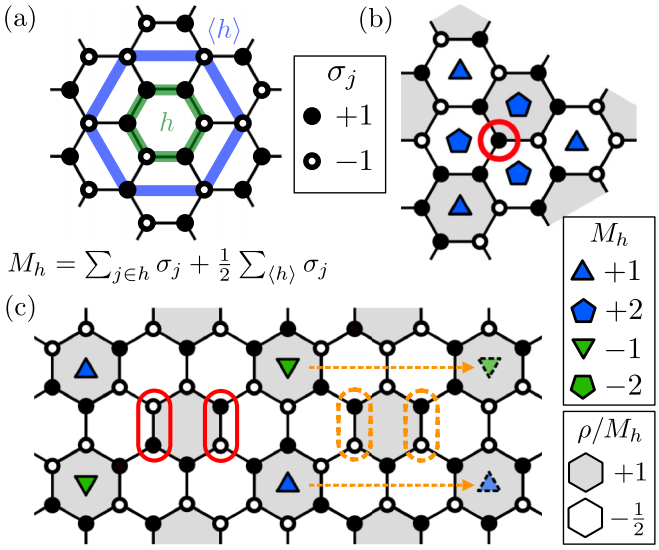

FIG. 1. Ground states of the honeycomb model fulfill the constraint $M_h = 0$, illustrated in (a). A single spin flip, as indicated by a red circle in (b), preserves total charge ρ as well as all dipole moments. The minimal-energy excitation, shown in (c) hence creates four distinct defects. These can be moved in pairs by flipping another four spins as indicated by orange dashed lines.

This allows numerical access to relatively large systems and low temperatures.

Simulating the model, we find that it exhibits a first order phase transition at low temperatures, but that the low temperature state nevertheless lacks signs of conventional order. Instead, the ground state correlations exhibit fourfold pinch points in momentum space, which are characteristic of systems described by a gauge theory of tensor fields [31].

Fractons in the honeycomb model. We consider an Ising model on the honeycomb lattice with Hamiltonian

$$H = \frac{J}{2}\sum_h M_h^2, \quad M_h = \sum_{j\in h}\sigma_j + \frac{1}{2}\sum_{j\in\langle h\rangle}\sigma_j, \tag{1}$$

which is a sum over constraints M_h, defined on hexagons h and their exteriors $\langle h\rangle$ as illustrated in Fig. 1(a).

A Hamiltonian of this form was first considered in Ref. [27] for $O(3)$ Heisenberg spins. There, it was shown that the system upon coarse graining can be described in terms of a suitably defined rank-2 tensor field m subjected to a generalized Gauss law

$$\partial_\mu\partial_\nu m^{\mu\nu} = \rho \tag{2}$$

with $\mathrm{Tr}[m] = 0$. It was also shown numerically that this emergent gauge theory is realized in its deconfined phase, that is, the system at low temperatures realizes a so-called higher-rank Coulomb phase.

While the mapping between the microscopic model and the coarse-grained field $m^{\mu\nu}$, discussed in detail later, generalizes to the Ising model [36], it is an entirely open question whether the system still realizes a higher-rank Coulomb phase, or whether restricting the degrees of freedom to be discrete yields a set of ground states, the average over which no longer corresponds to the deconfined phase of the gauge theory. For the case of the "conventional" Coulomb liquid, cases are known where the hard-spin Ising and Heisenberg behaviors are (e.g., pyrochlore [29]), and are not (e.g., kagome [32–35]), qualitatively similar to one another.

The components of the field m are formed by the local order parameter for antiferromagnetic order, with wave vector at the Brillouin Zone corners [27,36]. The Gauss law in Eq. (2) is then obtained by assuming a slow variation of m in real space and using a gradient expansion to turn the microscopic constraints on the spin configuration, M_h, into constraints on the spatial variation of $m_{\mu\nu}$. As a result, the relationship between the charge ρ and the microscopic constraint M_h breaks lattice symmetry by hand. We choose a subset of hexagons such that each site is a member of exactly one of them. One possible choice is illustrated in Fig. 1 by a darker shade of some hexagons. Denoting this subset as + hexagons and the rest as −, the charge is then defined as

$$\rho = \begin{cases} M_h & h \text{ is } + \text{ hexagon} \\ -\frac{1}{2}M_h & h \text{ is } - \text{ hexagon} \end{cases}. \tag{3}$$

Charges and moments of the higher-rank gauge theory can be determined explicitly from the microscopic model. The single spin flip, shown in Fig. 1(b), preserves both total charge ρ and the dipole moments $d^\nu = r^\nu\rho$. The lowest order moment of the charge distribution which changes is the quadrupole moment $q^{\mu\nu} = r^\mu r^\nu\rho$.

An excitation with the lowest (nonzero) energy of Eq. (1) involves four defects (hexagons with $M_h = \pm 1$); it can be constructed from four spin flips, Fig. 1(c). These defects are fractons: no single defect can be moved by any local combination of spin flips since that would change the total dipole moment. Pairs of (oppositely charged) fractons are lineons since they can be moved in the direction perpendicular to their dipole moment by flipping another four spins on the next-next hexagon, as indicated in Fig. 1(c) in dashed orange. Generally, fractons in our model appear at the corners of a "membrane" of flipped bonds. Fracton models are typically classified as 'type I' or "type II" based on how the fractons are created from the ground state and the mobility of fracton bound states [8]. In type I models the fractons appear at the corners of membranes and can form mobile bound states such as lineons, in type II models they appear on fractal structures and there are no mobile bound states. The model discussed here is type I, as can be seen from Fig. 1.

Extensive ground-state degeneracy. For periodic boundary conditions, the fact that pairs of fractons are lineons already implies a ground state entropy scaling at least subextensively ($\propto L$, where L is the linear system size): we can create a pair of lineons, move one of them around the system in a nontrivial way, and annihilate the pair again, reaching a different ground state [37]. In addition to moving a lineon in a particular direction, we can also split it into two, as shown in Fig. 2(a). Note that such a move is only possible because of sixfold rotation symmetry and would not be possible with cubic symmetry and more generally in the absence of at least three distinct orientations for the membranes. Crucially, in our case it can be done in two ways which we call forward and backward split, shown on the left and right of Fig. 2(a), respectively. The backward split is particularly important since it allows

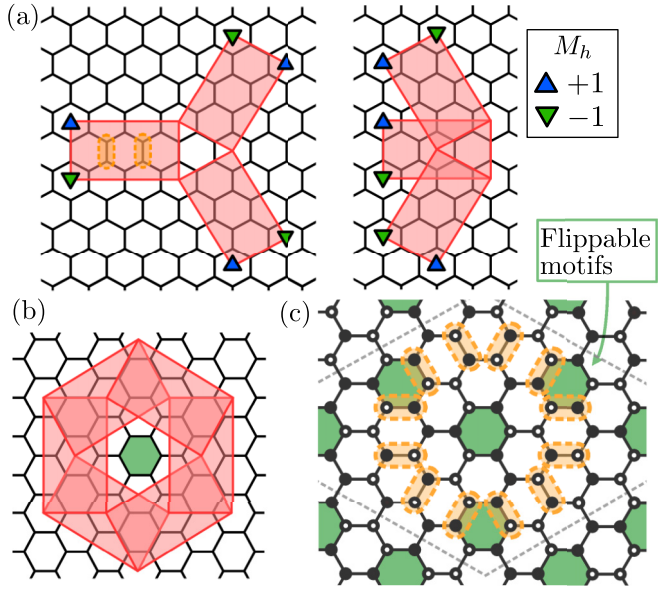

FIG. 2. Splitting of lineons and local resonance moves. (a) Pairs of fractons form lineons, mobile along a one-dimensional submanifold. These lineons can split in two, either the forward (left) or backward (right) directions. (b) A local combination of six membranes, can create, split, and recombine lineons, in such a way as to reach a new ground state configuration. This amounts to flipping 24 spins. Application of this move to the ground state in (c) does not create any excitation and could be centered around any of the green shaded hexagons. The move can be understood as a local combination of six membranes as shown in (b), where each corner overlaps with exactly one other corner of opposite charge.

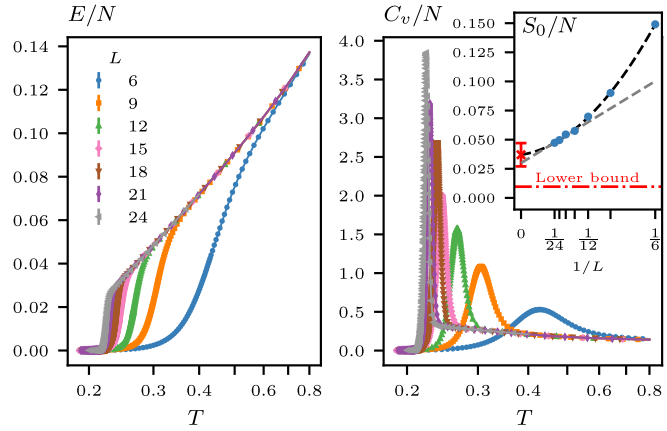

FIG. 3. Thermodynamics of the fractonic Ising model. Energy E and specific heat C_v from Monte Carlo simulation. Data is consistent with a first-order transition from a high-temperature paramagnetic phase to a low-temperature phase where the constraint $M_h = 0$ is satisfied. Inset: finite-size extrapolation of the ground state entropy per site.

us to close the worldline of lineons locally, resulting in a local move between different ground states. The minimal such move is shown in Figs. 2(b) and 2(c) and is a combination of six membranes [panel (b)] such that each corner defect is annihilated with exactly one other corner of opposite charge. This corresponds to flipping 24 spins simultaneously, as indicated in dashed orange in panel (c). There, we also explicitly show a ground state [36] with a finite density of such flippable motifs. The 24-spin move as shown in Fig. 2(c) could be centered on any of the hexagons colored in green, and nonoverlapping motifs can be flipped independently. Noticing that there is one idependently flippale motif per 72-site cell [indicated in Fig. 2(c) by a gray dashed line], establishes a number of ground state exponentials in the number of sites $N = 2L^2$ and in particular implies a lower bound on the residual entropy that scales extensively:

$$S_0 \geqslant \frac{N}{72} \log(2). \tag{4}$$

Cluster Monte Carlo algorithm. It is well established that in the presence of fracton excitations, any local algorithm will have a rapidly diverging relaxation time at low temperature [1,2,5]. Since single defects are immobile, local algorithms generally fail to anneal them out at low temperature and to gain access to the thermodynamics of Eq. (1), clearly a cluster algorithm is desirable. We have designed such an algorithm, which moves pairs of defects by effectively attempting to span one row of a membrane as shown in Fig. 1(c). In the crucial step, the algorithm starts by flipping two bonds on a single hexagon and accepting this move with metropolis probability. In the case that the move is rejected, the algorithm attempts to flip another four spins [as indicated in dashed orange in Fig. 1(c)], again trying to accept the move with metropolis probability, multiplied by a factor to account for the probability of rejecting the first move. This additional factor is needed to ensure detailed balance [38]. This is repeated until either the cluster is accepted or is ultimately rejected while spanning the full (linear) system size. If the move is accepted with zero energy cost, it either moves a distant pair of defects by one step in the direction perpendicular to the long side of the (single-row) membrane or it changes the ground state sector. While the relaxation time of this algorithm still scales significantly with system size at low temperature (we estimate $\tau \sim L^{7.4}$), it constitutes a major improvement over local dynamics [36]. When augmented with the local 24-spin move shown in Figs. 2(b) and 2(c), accepted with metropolis probability, and using feedback-optimized parallel tempering [39], we are able to equilibrate systems with up to $N = 1152$ ($L = 24$) spins in the ground state regime. To ensure equilibration, we compute the specific heat both directly from energy fluctuations and also as the derivative of internal energy with respect to temperature, and verify that these two estimators agree (cf. Fig. 3). This is considered a "stringent criterion" and is used, for example, in computational studies of model glass formers [40].

Thermodynamic properties and low-temperature correlations. We use the setup described in the previous paragraph to study the thermodynamic properties of Eq. (1) as a function of temperature for a range of system sizes as shown in Fig. 3. Both internal energy and specific heat are compatible with a first-order transition from a high-temperature paramagnetic phase to a low-temperature phase corresponding to the ground state regime $\langle E \rangle \approx 0$. Extrapolating the transition temperature to the thermodynamic limit yields an estimate of $T_c = 0.203 \pm 0.020$ [36]. Integrating the specific heat from high temperature yields an estimate of the residual

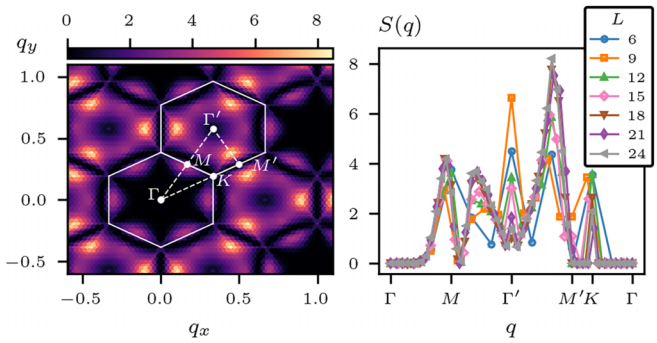

FIG. 4. The structure factor in the low-temperature phase at the system sizes studied shows no sharp features except clearly visible fourfold pinch points. These pinch points are the signature of an emergent higher-rank Gauss law [31] and are of the same form as found for a higher-rank spin liquid in a related continuous spin model [27].

entropy per site S_0/N for each system size. Fitting the system size dependence using both a linear fit to the last four sizes and a quadratic fit to all system sizes yields an estimate of $S_0/N = 0.037 \pm 0.010$. This is quite a bit above the lower bound derived above [Eq. (4)], but also comes with a large error bar due to significant finite size effects. The presence of these even at relatively large system sizes is not surprising given the size of the smallest local move as shown in Figs. 2(b) and 2(c).

Finally, we show the structure factor $S(\mathbf{q}) = \sum_{ij} e^{-(\mathbf{r}_i - \mathbf{r}_j)\cdot\mathbf{q}} \langle \sigma_i \sigma_j \rangle$ within the low-temperature phase in Fig. 4. It is fully consistent with a low-temperature higher-rank Coulomb phase since it shows no sharp features except fourfold "pinch-point" singularities at the zone boundaries, which are known to be a direct momentum-space signature of the generalized Gauss's law in Eq. (2) [31].

The presence of a sharp transition as a function of temperature is not inconsistent with a low-temperature liquid phase since a first-order transition is always possible also between continuously connected phases, as demonstrated by the famous transition between gaseous and liquid water. An alternative possibility is that the low-temperature phase is a so called "fragmented liquid" [41]; that is, the set of ground states, although extensive, breaks some symmetry on average. A possible hint in this direction is that the maximum of the structure factor along the line cut shown in Fig. 4 scales roughly with linear system size. However, as discussed already above there are still significant finite size effects. Ultimately, it is impossible to exclude the possibility of fragmentation in the absence of a more efficient algorithm and we leave this question open for future studies.

Conclusion. In summary, we have demonstrated the appearance of a fractonic spin liquid in the low temperature state of an Ising model on the honeycomb lattice. This low temperature state is separated from the high temperature paramagnet by a first order phase transition, and exhibits correlations matching those predicted for a Coulomb phase of rank-2 electric fields with scalar charges [31]. Elementary excitations are type I fractons, appearing at the corners of membranes of flipped spins.

The discovery of a relatively simple Ising model, with finite-range, two-body interactions establishes a useful platform for the further exploration of fractonic physics. This could include the perturbative introduction of quantum effects via transverse fields or transverse exchange. This may be a better setting in which to study quantum effects on fractons than in the Heisenberg models suggested in Ref. [27], for which numerical calculations suggest that quantum fluctuations wash out the multifold pinch points [42]. Here, the emergent Gauss's law is protected by a finite gap, so it may be more robust. Even if instanton effects drive the emergent gauge theory into a confined phase [as they do for the ordinary U(1) gauge theory in 1 + 1 D], the low temperature physics can still show interesting features related to the liquid phase.

Our purpose-built Monte Carlo algorithm provides a template for future numerical studies of type I fractonic models. Our algorithm, or its descendants, may also prove useful in the study of dynamical properties of such systems, addressing in more detail the topics of relaxation and disorder-free glassiness. The successful demonstration of an Ising fracton spin liquid, based on a Hamiltonian originally constructed for continuous spins [27], also raises the question of whether other classical spin liquids with higher-moment conservation laws [43,44] have Ising realizations, and what their properties may be.

Physical simulation platforms based on Rydberg atoms and superconducting qubits may be the most promising route to realization of our model. The model has the advantage of requiring only two-body interactions and, while it does require a fine tuning of interactions at different distances, the basic requirement for strong interactions which extend up to a finite cut-off distance is similar to models for Rydberg atom arrays [45,46]. Similar constraint structures have also been discovered recently in models for strongly interacting electrons in twisted-bilayer graphene [47]. We are therefore hopeful that the fractonic spin liquid uncovered here can be explored in the laboratory in the near future.

Acknowledgments. This work was in part supported by the Deutsche Forschungsgemeinschaft under Grant SFB 1143 (Project-Id 247310070) and the cluster of excellence ct.qmat (EXC 2147, Project ID 390858490).

[1] M. E. J. Newman and C. Moore, Phys. Rev. E **60**, 5068 (1999).
[2] C. Chamon, Phys. Rev. Lett. **94**, 040402 (2005).
[3] S. Bravyi, B. Leemhuis, and B. M. Terhal, Ann. Phys. **326**, 839 (2011).
[4] S. Bravyi and J. Haah, Phys. Rev. Lett. **111**, 200501 (2013).
[5] C. Castelnovo and C. Chamon, Philos. Mag. **92**, 304 (2012).
[6] B. Yoshida, Phys. Rev. B **88**, 125122 (2013).
[7] S. Vijay, J. Haah, and L. Fu, Phys. Rev. B **92**, 235136 (2015).
[8] S. Vijay, J. Haah, and L. Fu, Phys. Rev. B **94**, 235157 (2016).
[9] J. Haah, Phys. Rev. A **83**, 042330 (2011).

[10] M. Pretko, X. Chen, and Y. You, Int. J. Mod. Phys. A **35**, 2030003 (2020).
[11] R. M. Nandkishore and M. Hermele, Annu. Rev. Condens. Matter Phys. **10**, 295 (2019).
[12] C. Xu, Phys. Rev. B **74**, 224433 (2006).
[13] C. Xu and P. Hořava, Phys. Rev. D **81**, 104033 (2010).
[14] M. Pretko, Phys. Rev. B **95**, 115139 (2017).
[15] M. Pretko, Phys. Rev. B **96**, 035119 (2017).
[16] M. Pretko, Phys. Rev. D **96**, 024051 (2017).
[17] M. Pretko and L. Radzihovsky, Phys. Rev. Lett. **120**, 195301 (2018).
[18] J. Sous and M. Pretko, npj Quantum Mater. **5**, 81 (2020).
[19] Y. You, Z. Bi, and M. Pretko, Phys. Rev. Res. **2**, 013162 (2020).
[20] M. Pretko, Phys. Rev. B **100**, 245103 (2019).
[21] M. Hering, H. Yan, and J. Reuther, Phys. Rev. B **104**, 064406 (2021).
[22] H. Yan and J. Reuther, Phys. Rev. Res. **4**, 023175 (2022).
[23] N. E. Myerson-Jain, S. Yan, D. Weld, and C. Xu, Phys. Rev. Lett. **128**, 017601 (2022).
[24] K. Giergiel, R. Lier, P. Surówka, and A. Kosior, Phys. Rev. Res. **4**, 023151 (2022).
[25] S. Han, A. S. Patri, and Y. B. Kim, Phys. Rev. B **105**, 235120 (2022).
[26] H. Yan, O. Benton, L. D. C. Jaubert, and N. Shannon, Phys. Rev. Lett. **124**, 127203 (2020).
[27] O. Benton and R. Moessner, Phys. Rev. Lett. **127**, 107202 (2021).
[28] E. Z. Zhang, F. L. Buessen, and Y. B. Kim, Phys. Rev. B **105**, L060408 (2022).
[29] S. V. Isakov, K. Gregor, R. Moessner, and S. L. Sondhi, Phys. Rev. Lett. **93**, 167204 (2004).
[30] H. Yan, Phys. Rev. B **99**, 155126 (2019).
[31] A. Prem, S. Vijay, Y.-Z. Chou, M. Pretko, and R. M. Nandkishore, Phys. Rev. B **98**, 165140 (2018).
[32] I. Syozi, Prog. Theor. Phys. **6**, 306 (1951).
[33] K. Kanô and S. Naya, Prog. Theor. Phys. **10**, 158 (1953).
[34] D. A. Garanin and B. Canals, Phys. Rev. B **59**, 443 (1999).
[35] G.-W. Chern and R. Moessner, Phys. Rev. Lett. **110**, 077201 (2013).
[36] See Supplemental Material at http://link.aps.org/supplemental/10.1103/PhysRevB.110.L020401 for a brief review of the mapping to a higher rank gauge theory, construction of zero-energy moves, more detailed explanation and performance analysis of the cluster algorithm, as well as extended data.
[37] Moving a lineon [Fig. 1(c)] nontrivally around the system flips a row of spins at no energy cost and hence is reminiscent of the subsystem symmetries discussed in the context of other fracton models [7,48]. Note, however, that the move is not a symmetry of the Hamiltonian, but instead an emergent symmetry of a particular set of low-energy states. Furthermore, the ability to split, and locally recombine, lineons [Fig. 2] makes the situation here quite different from those of standard subsystem symmetries. Our model is also different from the discretizations of so-called higher-form Gauge theories [49,50], where excitations appear along the whole perimeter of the membrane and not just at the corners.
[38] *Advances in Computer Simulation*, edited by J. Kertesz and I. Kondor, Lecture Notes in Physics (Springer Verlag, 1998).
[39] H. G. Katzgraber, S. Trebst, D. A. Huse, and M. Troyer, J. Stat. Mech. (2006) P03018.
[40] L. Berthier and D. R. Reichman, Nat. Rev. Phys. **5**, 102 (2023).
[41] M. E. Brooks-Bartlett, S. T. Banks, L. D. C. Jaubert, A. Harman-Clarke, and P. C. W. Holdsworth, Phys. Rev. X **4**, 011007 (2014).
[42] N. Niggemann, Y. Iqbal, and J. Reuther, Phys. Rev. Lett. **130**, 196601 (2023).
[43] H. Yan, O. Benton, R. Moessner, and A. H. Nevidomskyy, arXiv:2305.00155.
[44] H. Yan, O. Benton, A. H. Nevidomskyy, and R. Moessner, arXiv:2305.19189.
[45] F. M. Surace, P. P. Mazza, G. Giudici, A. Lerose, A. Gambassi, and M. Dalmonte, Phys. Rev. X **10**, 021041 (2020).
[46] R. Verresen, M. D. Lukin, and A. Vishwanath, Phys. Rev. X **11**, 031005 (2021).
[47] D. Mao, K. Zhang, and E.-A. Kim, arXiv:2211.11622.
[48] D. T. Stephen, A. Dua, J. Garre-Rubio, D. J. Williamson, and M. Hermele, Phys. Rev. B **106**, 085104 (2022).
[49] A. E. Lipstein and R. A. Reid-Edwards, J. High Energy Phys. 09 (2014) 034.
[50] D. A. Johnston, Phys. Rev. D **90**, 107701 (2014).